PROCESSING OF UAV BASED RANGE IMAGING DATA TO GENERATE DETAILED ELEVATION MODELS OF COMPLEX NATURAL STRUCTURES

T.K. Kohoutek & H. Eisenbeiss

Institute of Geodesy and Photogrammetry, ETH Zurich, 8093 Zurich, Switzerland – tkohoutek@ethz.ch

Commission I, WG I/V

KEY WORDS: RIM, UAV, tracking, differential GNSS, mapping, DEM/DTM

ABSTRACT:

Unmanned Aerial Vehicles (UAVs) are more and more used in civil areas like geomatics. Autonomous navigated platforms have a great flexibility in flying and manoeuvring in complex environments to collect remote sensing data. In contrast to standard technologies such as aerial manned platforms (airplanes and helicopters) UAVs are able to fly closer to the object and in small-scale areas of high-risk situations such as landslides, volcano and earthquake areas and floodplains. Thus, UAVs are sometimes the only practical alternative in areas where access is difficult and where no manned aircraft is available or even no flight permission is given. Furthermore, compared to terrestrial platforms, UAVs are not limited to specific view directions and could overcome occlusions from trees, houses and terrain structures. Equipped with image sensors and/or laser scanners they are able to provide elevation models, rectified images, textured 3D-models and maps.

In this paper we will describe a UAV platform, which can carry a range imaging (RIM) camera including power supply and data storage for the detailed mapping and monitoring of complex structures, such as alpine riverbed areas. The UAV platform NEO from Swiss UAV was equipped with the RIM camera CamCube 2.0 by PMD Technologies GmbH to capture the surface structures. Its navigation system includes an autopilot. To validate the UAV-trajectory a 360° prism was installed and tracked by a total station.

Within the paper a workflow for the processing of UAV-RIM data is proposed, which is based on the processing of differential GNSS data in combination with the acquired range images. Subsequently, the obtained results for the trajectory are compared and verified with a track of a UAV (Falcon 8, Ascending Technologies) carried out with a total station simultaneously to the GNSS data acquisition. The results showed that the UAV's position using differential GNSS could be determined in the centimetre to the decimetre level. The RIM data indicated a high noise level in the measured distance image, due to the vibrations caused by the flight system. Multi-image processing reduced the noise level of the distance image. The produced elevation models from a test area show the high potential of the proposed method for complex structures such as riverbeds.

1. INTRODUCTION

Several geodetic and environmental applications deal with accurate reconstruction of the geometry of surface measurements in three dimensional (3D) models. Those high quality surface models can help to advance the understanding of earth surface processes. Photogrammetry and laser scanning have become widely used, and specialized workflows have been developed to obtain those 3D data at various scales in diverse environments.

Terrestrial laser scanning (TLS) has proved to be a rapid and precise survey technique. However, by vegetation cover, uneven and/or steep terrain and difficult accessibility it comes to its limits. Photogrammetry instead needs good contrasts in a scene to identify the same features in a minimum of two images to measure their displacement. Hereby the ambient light level and spatial distribution of the target's reflectivity have an impact on the performance of photogrammetry systems (Sackos et al. 1996).

Objects (e.g. boulders) in the line of sight obscure the surface, even when the camera/scanner is placed at different points. The need of a good accessibility, an elevated position and a free line of sight makes it difficult to use TLS under hazardous environmental conditions (Marszalec et al. 1995). Acquiring data from the bird's eye perspective can minimize those shadowing effects. This can be obtained by mounting the capturing device on poles (Bird et al. 2010) or kites (Giménez et al. 2009), even below the canopy, where airborne or satellite images are not feasible. In our approach the capturing device is mounted on an UAV.

The capturing device in the presented work is a RIM camera. RIM techniques were tested and reviewed already in the 1980s by Jarvis (1983) and Besl (1988). Kolb et al. (2010) gave a more recent overview of RIM cameras. The suitability and accuracy in centimetre do decimetre level of RIM cameras for scientific measurements have been evaluated mostly for indoor applications (e.g. Dorrington et al. 2010). The outdoor usage of RIM cameras is described in a few publications, e.g. for cultural heritage studies (Chiabrando et al. 2010) and the measurement of canopy density (Schulze 2010). Our application is based on the measurements of streambed morphology (Nitsche et al. 2010, Nitsche et al. 2012) when the used RIM camera was mounted on a lightweight crane. The acquired 3D point clouds have been registered by connecting points that have been measured in a global coordinate system for georeferencing of the scene.

In our application the on-board GNSS/INS (global navigation satellite system and inertial navigation system) is used to track the position and orientation of the UAV and register the point clouds by the flight pass without additional artificial targets. To qualify the accuracy of the on-board positioning system, the

UAV will be equipped also with a 360° prism. A total station will track the flight pass to compare the data with the on-board units.

2. TECHNOLOGIES: UAVS AND RIM

2.1 Requirements on the technologies

UAV and RIM systems need certain factors and environmental conditions to work properly. The operation of UAVs is limited through maximum payload, regulatory requirements, power supply and visibility to the UAV system as well as the respectability of the GNSS signal. Furthermore, the UAV as a measurement system is restricted through vibrations during the flight and the camera gimbal configuration.

On the other hand RIM cameras are mainly influenced by light conditions, distance to the object and its reflectance. Furthermore the camera needs a power supply and a computer to store the acquired data.

2.2 UAVs

UAVs are inhabited, reusable motorized aerial vehicles. These systems can fly autonomously, semi-autonomously or manually steered by a pilot from the ground using a remote control. Instead of the aberration UAV synonyms like UAS (Unmanned Aircraft System) and UVS (Unmanned Vehicle System) can be found in the literature (Eisenbeiss 2009).

UAVs can be used as mapping platforms. These platforms are equipped with photogrammetric measurement systems, including, but not limited to small or medium size still-video or video cameras, thermal or infrared camera systems, multispectral cameras, RIM and airborne LiDAR sensors, or a combination thereof depending on the payload of the UAV. Furthermore, for the determination of the trajectory, UAVs feature by default an integrated GNSS/INS system, barometric altimeter and compass systems.

The combination of aerial and terrestrial photogrammetry allows UAVs to generate a wide field of possible applications in the close range domain. Furthermore, UAVs introduce new (near-) real time applications and low-cost alternatives to the classical manned aerial photogrammetry.

An overview about UAV applications in photogrammetry is given in the proceedings of the UAV-g conference 2011 (Eisenbeiss et al. 2011).

2.3 RIM

RIM cameras, based on the Time of Flight (ToF) principle, use an amplitude-modulated continuous light emitter along with a CCD/CMOS receiver. It is a young but quickly developing technology. The sensor samples the reflected light regularly four times with an internal phase delay (Lindner et al. 2009) and calculates the correlation amplitude and the incident light intensity as well as the phase shift of the modulation (Möller et al. 2005). Finally the measured distance can be calculated and the direct output of Cartesian 3D coordinates is possible.

Several calibration approaches for RIM cameras have been developed to compensate intrinsic error sources like temperature and lens distortion (e.g. Kahlmann and Ingensand 2005 and Westfeld et al. 2009). The quality of single distance measurements clearly varies with ambient light conditions

(Nitsche et al. 2010). A single range image is very noisy and data quality has to be enhanced by averaging images of the same footprint.

3. FIELD WORK

3.1 Preparation

The unmanned helicopter NEO S-300 prototype by Swiss UAV was equipped with the TOF camera CamCube 2.0 (Table 1). This NEO prototype operates without a shell and allows the quick attachment and modification of the measurement equipment. It can be controlled manually, assisted or completely autonomous using the wePilot (weControl, 2012) auto pilot and is able to lift up the equipment, including RIM camera, Netbook and batteries of about 5 kg in total. In addition to the RIM camera, a 360° prism was mounted on the UAV to track the helicopters' position with a total station and compare the data with the on-board GNSS (Figure 1).

Table 1 Specifications of RIM camera

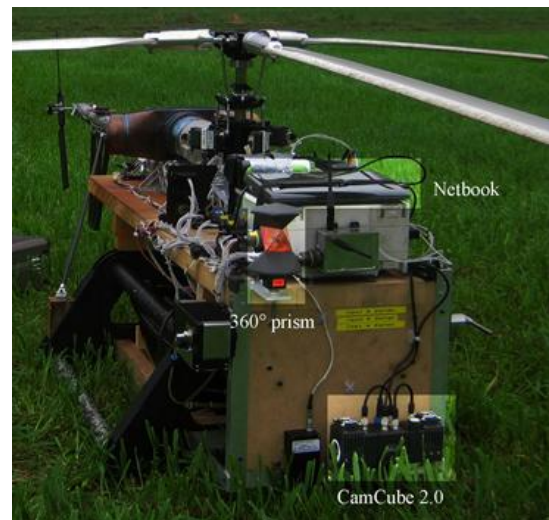| Model	CamCube 2.0
Modulation frequency (MHz)	18 - 21
Unambiguous measurement range (m)	0.3 - 7.5
Sensor pixels	204 x 204
Field of view (degree)	40 x 40
Mean resolution at 3 meter (mm)	10.7
Footprint area at 3 meter (m^2)	4.77
Camera weight (g)	1370
Camera dimensions (mm)	180 x 194 x 180
Frame rate (f/s)	25
Illumination wavelength (nm)	870

Figure 1: Experimental NEO platform with sensors (Kohoutek et al. 2011)

A test field was created to verify the resolution of the RIM camera at different flight heights (Kohoutek et al. 2011). The objects used in the test field (Figure 2) varied in size, shape and material, like spheres ($\varnothing$ = 12 and 15 cm, material: wood), cylinders (height = 5 cm, material: rubber), lumbers (material: wood), a box (40 x 25 x 15 cm, material: plastic) and cones (height ~40 cm, material: plastic).

Figure 2: Test field objects

3.2 Data acquisition

The energy supply was one of the practical challenges of the RIM camera mounted on the UAV system. To support an operating window of ~10 minutes several 12 V/2 Ah batteries were attached on the helicopter. Another problem was the standard netbook that was used to acquire the range data. Unfortunately, the mechanical hard disk stopped working due to the vibrations of the helicopter's jet engine. Consequently another netbook with a solid-state disk (SSD) was mounted on the helicopter. Although the SSD was not influenced through the vibrations of the UAV system, the processor of the second netbook was not powerful enough to acquire the data with a sufficient frequency.

During data acquisition, the NEO was steered in the assisted flight mode, hovering in three height levels of 3 m, 5 m and 7 m above the ground, limited by the ambiguity range of the TOF sensor of ~7.5 m. A total station tracked its path to verify the accuracy of the on-board single antenna GPS that coordinates have been logged during the flight. Furthermore the data logger captured the pitch, yaw and tilt angles of the INS.

3.3 Lessons learned

As mentioned in chapter 2.3, a single range image is very noisy. Due to the low processor power there have been only 4 frames per second (f/s) captured during the flight instead of a normal acquisition rate of 16 - 25 f/s. We assume that the low processor power also influenced the data logger. It turned out that the log files have been incomplete, disrupted or even empty and could not been used to analyse the helicopter's GPS accuracy.

4. ANALYSIS OF THE FLIGHT TRAJECTORY

Because of the previously mentioned problems of the data logger of the NEO platform, the measurement setup of an UAV equipped with a 360° prism was repeated at the ETH Zurich with smaller UAV system. The flight test was done using autonomous flight mode of the UAV, since we tried to have similar conditions as we had during the tracking with the NEO S-300. However, the tracking of a comparable helicopter and the comparison with results from integrated autopilot (wePilot) were published in Eisenbeiss et al. (2009). In this study the absolute accuracy of the GNSS data (single frequency receiver) was in meter level, while the relative accuracy of the flight trajectory is in the decimetre level.

4.1 Methods for the determination of the UAV flight trajectory

Preliminary works with respect to UAV tracking were conducted in Eisenbeiss (2009) and Eisenbeiss et al. (2009). In these studies first investigations related to UAV tracking and the analysis of the UAV trajectory (model helicopter copter 1B) were investigated. The work presented in this paper occurred based on several projects, which were accomplished with the UAV system Falcon 8 at the IGP (Institute of Geodesy and Photogrammetry) at ETH Zurich. However, the orientation of the Falcon 8 system was not focus of this study. Investigation combining evaluation with respect to the UAV position and orientation are published in Niemeyer et al. (2012).

4.2 Accuracy analysis of the UAV flight trajectory

4.2.1 Differential-GPS Trajectory

The GPS raw data are provided in the binary format of µ-blox (Falcon 8) and Leica (reference station). With regard to the differential post-processing in two different software packages, the data was converted into the RINEX (Receiver Independent Exchange) format. The differential post-processing of the GPS data was carried out with the software package GrafNav.

Concerning the verification with the track it was further necessary to adjust the frequencies of the data set. In the following only the 1 Hz frequency for the analysis is taken into account. The achieved accuracies of the internal GrafNav solutions are less than one decimetre (Bláha et al. 2011).

4.2.2 Tracking with the total station

The Falcon was tracked with a total station. Thereby a Leica SmartStation was applied as measuring instrument. Since the tracking data of the Leica TPS1201 features a high accuracy (millimetre and centimetre level for tracking modus) it is suited as reference data of the differentially processed GPS data. For the tracking with the SmartStation, it was necessary to fix a reflector (Leica 360° mini prism) on the mounting system of the octocopter (Figure 3). However, due to the payload limitations, the camera mounted on the gimbal was removed during the tracking of the Falcon 8 system.
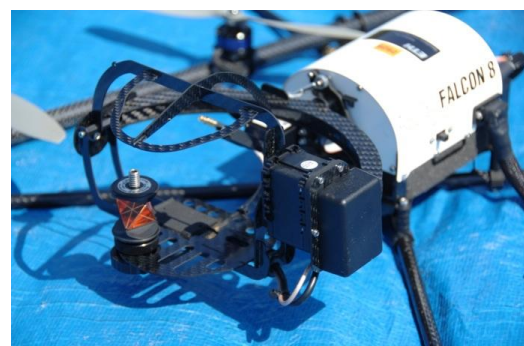

Figure 3: Gimbal of the Falcon 8 system equipped with a 360° mini prism from Leica Geosystems (Bláha et al. 2011)

4.2.3 Comparison of the trajectories

The two trajectories (SmartStation and GPS UAV) were compared in Matlab. The mean offset of the total trajectory is 0.8 m with a standard deviation of 0.45 m. A mean 3D

difference of 0.3 m with a standard deviation of 8 cm was achieved for one flight line (see Figure 4, red part of the trajectory). This offset mainly comes from the offset between the GPS antenna and the 360° mini prism. Variable sampling frequency of the total station influenced mainly the accuracy of the turning parts of the trajectory.
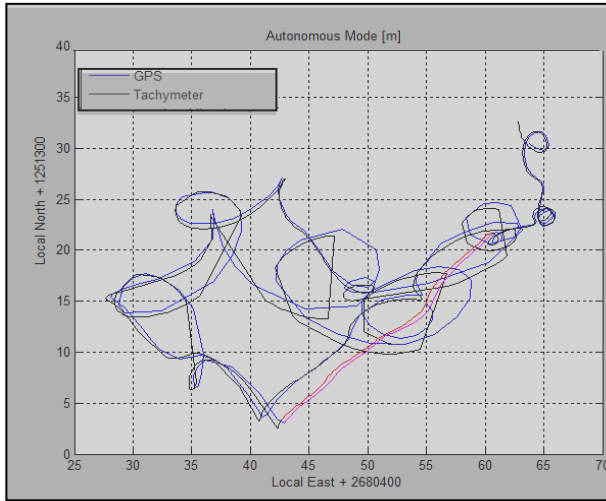

Figure 4: 2D-Plot of the registered trajectories. The analysis of one flight line is highlighted in red

Furthermore, the result of the GPS trajectory is also influenced by the GPS post-processing. The ambiguities of the phase measurements were not completely solved during the flight, thus it is expected that the internal accuracy given in 4.2.1 are too optimistic. However, the results from the new GPS antenna (u-blox LEA 6T) integrated into the Falcon 8 system are more robust in the comparison to the experiments published in Bláha et al. 2011. From the results given above it could be expected to achieve similar results for the processing of GPS data of the Swiss UAV system in possible future studies.

5. PROCESSING AND ANAYLSIS OF THE RANGE DATA

Several internal error sources (e.g. originating from the optical system and the semiconductor technology itself) and environmental factors (e.g. multiple reflections and surface reflectivity properties) influence the RIM data. A good overview is given in Nitsche et al. (2012), yet there is no error model for RIM noise established (Lindner *et al.* 2010). In laboratory experiments with the CamCube 2.0 at the ETH Zurich a distance accuracy of 2-23 mm was determined for measurements on a highly reflective flat surface. For favourable field conditions the distance accuracy can be worse a factor of 2-3.

Due to the low frame rate mentioned in chapter 3.3 an average image for useful noise reduction of the region of interest could not been calculated. Furthermore, occurring motion artefacts have not been considered. They arise from unmatching phase values during the demodulation process where objects or the camera itself move. The presented approach from Lindner et al. (2009) to use the Optical Flow to minimize those motion artefacts can be seen equivalent to the forward-motion-compensation from airborne photogrammetry. However, the test

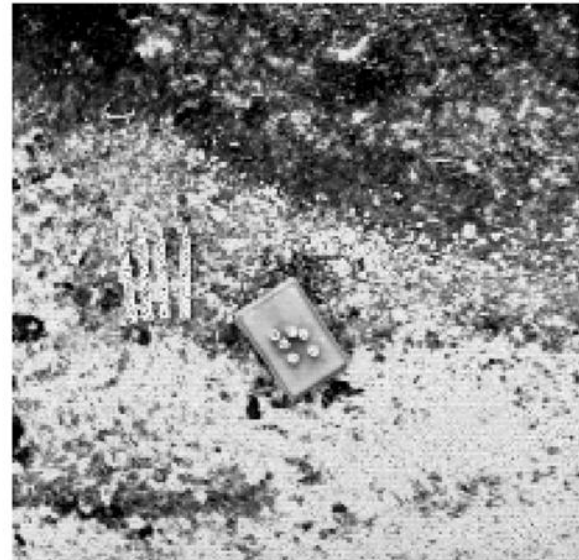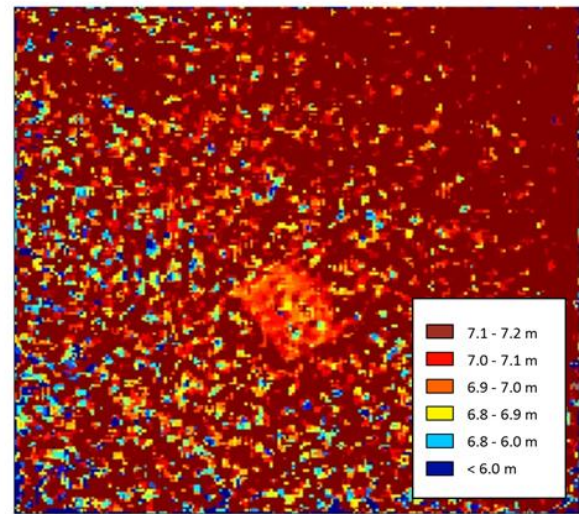field objects were detected in a single exposure during a flight height of 7.5 m (Figure 5).

Figure 5: Aerial range image (7.5 m flight height) (Kohoutek et al. 2011) top: median filtered single distance image, middle: single intensity image, bottom: single amplitude image

It can be seen that the median filtered range image shows only the plastic box object. Smaller objects, like the cones and wooden lumbers cannot be distinguished from the noise. Analysing the intensity image, where the intensity is a measure for the strength of the total light (ambient light + modulated light) the box with sharp borders and the small cones on top of it can be detected. However, the lumbers are only clearly visible in the amplitude image. The amplitude represents the measure for the modulation amplitude (i.e. the number of electrons per pixel generated by the incoming modulated light) (Lange et al. 1999).

We assume that a combination of amplitude and intensity image would raise the detection of objects in the point cloud by the definition of regions of interest. A higher precision could be achieved when measuring without ambient light. Nitsche et al. (2012) presented that random noise can be reduced effectively by taking the median of repeated measurements, which results in significantly reduced distance errors.

A direct georeferencing of the acquired point cloud can be realized by the captured GPS positions and the pitch, yaw and tilt angle of the UAV (Škaloud, 1999).

6. SUMMARY UND PERSPECTIVES

The fast and real time 3D data acquisition of static and kinematic objects is a main advantage of RIM cameras compared to laser scanning and photogrammetry. Furthermore, post-processing of RIM data is relatively fast and straightforward. However, one of the major drawbacks of RIM is the limited range of only up to 10 meter. TLS and some photogrammetric methods are better suited to achieve highly accurate data over long ranges. RIM could be considered an alternative for TLS or photogrammetric approaches in small-scale applications where kinematic 3D data is necessary. Positioning techniques like the GNSS/INS unit from UAVs can be exploited and combined with RIM measurements to obtain real-time referenced global coordinates for the acquired objects.

The comparison of the trajectories showed that with GPS post-processing the accuracy comes down to decimetre-level, which could be expected from the processing differential GPS using L1 frequency receiver. It is expected to improve the results by using two frequency receiver and differential GNSS data processing. For the analysis of the trajectory the results from the 3D trajectory could be compared in future studies using indirect georeferencing of images using ground control points or tracking of the UAV with a video-based SmartStation, were the UAV could be extracted in the video (Niemeyer et al. 2012).

The focus in the presented study was not on the orientation of the RIM images. However, Hartmann et al. (2012) present a promising method for the automated orientation of thermal images, which have a similar image resolution as RIM images. In future work the combined processing of differential GNSS and image data have a great potential for the automated processing of UAV image data (RIM and visible) for the generation of elevation models.

REFERENCES

Besl, P.J., 1988. „Active, optical range imaging sensors", Machine Vision and Applications (1), pp. 127-152.

Bláha, M., Eisenbeiss, H., Grimm, D. E. and Limpach, P., 2011. „Direct georeferencing of UAVs", Proceedings of the International Conference on Unmanned Aerial Vehicle in Geomatics (UAV-g), Vol. XXXVIII, Zurich, Switzerland.

Chiabrando, F., Piatti, D. and Rinaudo, F., 2010a. „Integration of tof camera and multi-image matching approach for cultural heritage survey", International Archives of Photogrammetry, Remote Sensing and Spatial Information Sciences, Commission V Symposium: Newcastle upon Tyne, UK.

Dorrington, A.A., Payne, A.D. and Cree, M.J., 2010. „An evaluation of time-of-flight range cameras for close range metrology applications", International Archives of Photogrammetry, Remote Sensing and Spatial Information Sciences, Commission V Symposium: Newcastle upon Tyne, UK.

Eisenbeiss, H., 2009. „UAV Photogrammetry", PhD thesis, ETH Zurich, Switzerland. DISS. ETH NO. 18515, doi:10.3929/ethz- a-005939264.

Eisenbeiss, H., Stempfhuber, W. and Kolb, M., 2009. „Genauigkeitsanalyse der 3D-Trajektorie von Mini-UAVs", Tagungsband der Deutschen Gesellschaft für Photogrammetrie und Fernerkundung (DGPF) 18/2009.

Eisenbeiss, H., Kunz, M., and Ingensand, H., 2011. „Proceedings of the International Conference on Unmanned Aerial Vehicle in Geomatics (UAV-g)", Vol. XXXVIII, Zurich, Switzerland.

Giménez, R., Marzolff, I., Campo, M.A., Seeger, M., Ries, J.B., Casali, J. and Álvarez-Mozos, J., 2009. „Accuracy of high-resolution photogrammetric measurements of gullies with contrasting morphology", Earth Surface Processes and Landforms, 34(14), pp. 1915-1926.

Hartmann, W., Tilch, S., Eisenbeiss, H., Schindler, K., 2012. „Determination of the UAV position by automatic processing of thermal images", The International Archives of the Photogrammetry, Remote Sensing and Spatial Information Sciences, ISPRS Congress, Melbourne, Australia, XXIX, (accepted).

Jarvis, RA., 1983. „A Perspective on Range Finding Techniques for Computer Vision", Ieee Transactions on Pattern Analysis and Machine Intelligence 5(2), pp. 122-139.

Kahlmann, T. and Ingensand, H., 2005. „Calibration and improvements of the high-resolution range-imaging camera SwissRanger TM", Conference on Videometrics VIII, part of the IS&T/SPIE Symposium on Electronic Imaging, Vol.5665, San Jose, USA.

Kahlmann, T. and Ingensand, H., 2007. „High-precision investigations of the fast range imaging camera SwissRangerTM", SPIE 6758-18, Optics East 2007, Boston, USA.

Kohoutek, T.K., Nitsche, M. and Eisenbeiss, H., 2011. „Geo-referenced mapping using an airborne 3D time-of-flight camera", ISPRS Laser Scanning Workshop, Calgary.

Kolb, A, Barth, E, Koch, R and Larsen, R., 2010. „Time-of-Flight Cameras in Computer Graphics" Computer Graphics Forum 29(1), pp. 141-159.

Lange, R., Seitz, P., Biber, A. and Schwarte, R., 1999. „Time-of-flight range imaging with a custom solid-state image sensor", Laser Metrology and Inspection. Proc. SPIE: Munich. pp. 180-191.

Lindner, M. and Kolb, A., 2009. „Compensation of Motion Artifacts for Time-of-Flight Cameras", Dynamic 3D Imaging, pp. 16-27.

Lindner, M., Schiller, I., Kolb, A. and Koch, R., 2010. „Time-of-Flight sensor calibration for accurate range sensing", Computer Vision and Image Understanding 114(12), pp. 1318-1328.

Marzalec, J., Myllylä, R. and Lammasniemi, J., 1995. „A LED-array-based range-imaging sensor for fast three-dimensional shape measurements". Sensor and Actuators A. Vol. 46-47, pp. 501-505.

Niemeyer, F., Bill, R. and Grenzdörffer, G., 2012. „Konzeption und Genauigkeitsabschätzungen für eine Bestimmung der äußeren Orientierung eines Unmanned Aerial Vehicles (UAV)", PFG 2012 / 2, pp. 141–157.

Nitsche, M., Turowski, J.M., Badoux, A., Pauli, M., Schneider, J., Rickenmann, D. and Kohoutek, T.K., 2010. „Measuring streambed morphology using range imaging". River Flow 2010 - Dittrich, Koll, Aberle & Geisenhainer (eds) - Bundesanstalt für Wasserbau ISBN 978-3-939230-00-7.

Nitsche, M., Turowski, J.M., Badoux, A., Rickenmann, D., Kohoutek, T.K., Pauli, M. and Kirchner, J. W., 2012. „Range Imaging: a new method for high-resolution topographic measurements in small- and medium-scale field sites", Earth Surface Processes and Landforms, accepted.

Sackos, J., Bradley, B., Nellums, B. and Diegert, C., 1996. „The Emerging Versatility of a Scannerless Range imager". Sandia National Laboratories, Exploratory Systems Development and Parallel Science Computing Centers, Albuquerque, New Mexico, USA.

Schulze, M., 2010. „3D-camera based navigation of a mobile robot in an agricultural environment". International Archives of Photogrammetry, Remote Sensing and Spatial Information Sciences, Commission V Symposium: Newcastle upon Tyne, UK.

Škaloud, J., 1999. „Optimizing Georeferencing of Airborne Survey Systems by INS/DGPS". PhD thesis, Department of Geomatics Engineering, University of Calgary, Alberta.

WeControl, 2012. weControl corporate website, http://www.wecontrol.ch/, (accessed April 10 2012).

Westfeld, P., Mulsow, C. and Schulze, M., 2009. „Photogrammetric calibration of range imaging sensors using intensity and range information simultaneously". Optical 3-D Measurement Techniques IX. Vol. II, pp. 129.